Coordinated Control of PSS with Type-2 Fuzzy Lead Lag SSSC Damping Controller Design Using Modified Local Signal

Asit Kumar Patra[1] and **Sangram Keshori Mohapatra**[2†], Non-members

ABSTRACT

The Sine Cosine adapted improved WOA(SCiWOA) based design coordinated control of Type-2 fuzzy logic control (T2FLC) power system stabilizer (PSS) with modified local signal (MLS) input to Type-2 FLC lead-lag-based Static synchronous Series Compensator (SSSC) controller considered for transient stability improvement. Initially, the SCiWOA optimized coordinated control of MLS input to a lead lag-based SSSC controller with PSS was compared with the Whale Optimization Algorithm (WOA) and particle swarm optimization (PSO) based coordinated control of the same controller with the structure of the SMIB power system. It is seen from the demonstration that improvements in the ITAE error with the proposed SCiWOA tuned compared to WOA and PSO are 29.83% and 33.91%, respectively. The different input signals to PSS and SSSC coordinated control were verified to check the effectiveness and robustness of the analysis of the transient stability of the power system. The next part of the analysis attempted to coordinate the control of T2FLC based PSS with a T2 FLC controller with a remote input signal ($\Delta\omega$) based PSS with a lead-lag SSSC damping controller under different loading and fault conditions of the SMIB power system. Lastly, the effectiveness of the proposed coordinated controller demonstrated in three machine power systems shows that the proposed T2FLC based PSS with MLS input-based T2FLC in the SSSC damping controller has superior transient performance as compared with PSS with MLS input to the SSSC controller and PSS with MLS input to the SSSC controller under three different contingencies of the power system.

Keywords: Type-2 FLC Lead Lag Controller, Type-2 FLC PSS, Sine Cosine Adapted Improved WOA (SCiWOA), Static Synchronous Series Compensator, Transient Stability

Manuscript received on December 1, 2022; revised on March 1, 2023; accepted on August 3, 2023. This paper was recommended by Associate Editor Yuttana Kumsuwan.

[1]The author is with Department of Electrical Engineering, Seemanta Engineering College, Mayurbhanj, Odisha, India.

[2]The author is with Department of Electrical Engineering, Govt. College of Engineering, Keonjhar, Odisha, India.

[†]Corresponding author: sangram.muna.76@gmail.com

Digital Object Identifier: 10.37936/ecti-eec.2023213.251468

1. INTRODUCTION

In the present day, demand for electricity increases; therefore, the interconnected power system network is heavily loaded, leading to major changes in complex power flow in the system and causing instability. It is a challenging and difficult task for power system operation and control under different operating conditions when disturbances occur in the interconnected power system. Due to the disturbances, the power system oscillates in the low frequency range, which affects the dynamic stability of the system. Therefore, it is very important to provide sufficient damping torque to suppress the low-frequency oscillations of the power system [1–2]. In past decades, the conventional PSS has been used to improve the reliability of the power system. The PSS damps out the oscillation of the system, but it is not efficient for large disturbances and needs a supplementary controller to improve the damping oscillation of the power system.

Fortunately, the development of power electronics Flexible Alternating Current Transmission System (FACTS) controllers has the potential to solve the problems of transient stability and dynamic stability margin in the power system. The FACTS controllers are widely used due to their faster control of both active and reactive power and enhanced transmission capacity of the existing line, which increases system security and reliability [3–4]. Static Series The synchronous compensator is a dominant series-connected device in the FACTS controller that controls the power flow in the transmission line. The SSSC has fast dynamic performances for controlling the voltage and current, which decrease the damping of the oscillations in the power system during disturbances [5]. A secondary stabilizing signal is superimposed in the SSSC control circuit for better transient performance. As most of the literature indicates, coordinated control of SSSC based controllers used in lead-lag controllers is considered for the transient stability of the different power systems. The proposed analysis is carried out by considering the coordinated control of a T2FLC based lead-lag SSSC damping controller with a power system stabilizer.

The literature survey reveals that traditional computational approaches are more time-consuming as their convergence rate is sluggish, and this requires a significant computational problem due to the iterative process. On the other hand, only local minima are emphasized by the search method, so the required solution may not

Nomenclature

MLS	Modified Local Signal	T2FLC	Type 2 Fuzzy Logic Control
SCiWOA	Sine Cosine Adapted Improved WOA	PSS	Power System Stabilizer
WOA	Whale Optimization Algorithm	LL	Lead Lag
PSO	Particle Swarm Optimization	SOC	Center of Sets
ITAE	Integral Time Absolute Error	PI	Proportional Integral
SSSC	Static Synchronous Series Compensator	MF	Membership Function
FACTS	Flexible Alternating Current Transmission System	LMF	Lower Membership Function
IGBT	Insulated Gate Bipolar Transistor	UMF	Upper Membership Function
PWM	Pulse Width Modulation	TR	Type Reducer
VSC	Voltage Source Converter	MOL	Many Optimizing Liaisons
GA	Genetic Algorithm	PID	Proportional Integral Derivative Control
DE	Differential Evolution	FO	Fraction Order
GSA	Gravitational Search Algorithm	SOA	Seeker Optimization Algorithm
BFOA	Bacterial Foraging Algorithm	ANFIS	Adaptive-network-based Fuzzy Inference System
FLC	Fuzzy Logic Control	FOU	Foot Print of Uncertainty
SF	Scaling Factors	EXN	Extreme Negative
LN	Least Negative	EXP	Extreme Positive
ZER	Zero	SMIB	Single Machine Infinite Bus
LP	Least Positive	DC	Direct Current
$\Delta\omega$	Remote Speed	PLL	Phase-Locked Loop
ΔP	Active Power	PL	Line Power
I	Current	M	Inertia Constant

be ideal. A lot of new optimization approaches focused on artificial intelligence have been proposed for the design of a power system stabilizer and a supplementary damping controller based on FACTS controllers. The SSSC based coordinated control design using different optimization techniques like particle swarm optimization [6], Genetic Algorithm (GA) [6–8], Differential Evolution (DE) [9], Gravitational Search Algorithm (GSA) [10–11], Bacterial foraging algorithm BFOA [12], hybrid-BFOA-PSO [13–14], hybrid DE-PSO [15], hybrid Neuro-fuzzy [16], ANFIS [17], SOA [18], and Novel Grey Wolf Optimization [19] has been attempted for the stability improvement analysis of the different types of power systems.

A hybrid firefly-swarm-based type-2-based fraction order (FO) fuzzy PID based power system stabilizer has been proposed for enhancement of power system stability in the power system [20]. The proper input signal selection is very important for the design of a stable damping controller in the power system. The input signal must be capable of monitoring proper action during a power system interruption. According to a literature survey, many researchers have taken remote and local signals as inputs to the controllers of different power systems. Most of the researchers reported that the remote signal is a better choice than the local signal [21] from a power system transient stability point of view. As the SSSC FACTS controller is installed in series with the transmission line, an additional cost is required for the communication of remote signals from the generator to the SSSC based controller. Although local signals are easily available their main demerit is that they cannot achieve the satisfactory damping of oscillations in the power system. This paper attempts the coordinated control of PSS with an SSSC based damping controller by considering a modified local signal as the input to the controller for the transient stability analysis. The BFOA-MOL approach to power systems used an MLS based lead-lag SSSC controller design for the analysis of stability enhancement in the power system [22].

The proposed article analyzed the SCiWOA, WOA, and PSO based optimized coordinated control of remote input ($\Delta\omega$) signals to PSS and MLS inputs to the lead-lag-based SSSC damping controller design for the SMIB power system considered for the transient stability analysis. From the study of SCiWOA optimized coordinated control, the best value of the ITAE objective function is obtained as compared to WOA and PSO optimized with the same control structure and power system. It also studies the coordinated control of SSSC control by employing different types of input signals in SSSC and PSS by using the WCiWOA optimized tuning parameter for transient stability improvement in the SMIB power system. As per the no free lunch (NFL) proposition, there is no technique that is fit for every problem. In this analysis, sine-cosine-adapted improved WOA has been proposed for the improvement of WOA. The anticipated SCiWOA technique can be obtained by using the scaling factors, which change the position of step size to update the search process of the original WOA [23]. The sine and cosine functions are engaged in defining the control parameter *'c'* of WOA in the optimization process. The proposed algorithm is employed to design a coordinated control of the remote input signal ($\Delta\omega$) of Type-2 Fuzzy

Logic PSS (T2FLC PSS) with modified local signal input to a Type-2 Fuzzy Logic Lead Lag (T2FLC LL) SSSC based damping controller for transient stability improvement of the power system. The proposed SCiWOA optimized coordinated control of T2FLC PSS with T2FLC LL SSSC controller (the scaling factor of both PSS and SSSC controller) help the upgrading factor for the best tuning parameters to be obtained for improving the transient performances of the power system. Based on the previous literature, this paper has attempted a new type of coordinated control of T2FLC based PSS with an SSSC based damping controller by using the Type-2FLC and considering the MLS input signal in the power system. In view of the above, the major contributions of the present work are as follows:

- The coordinated control of $\Delta\omega$ based input to PSS with MLS input to the lead-lag-based SSSC damping controller employs the SCiWOA, WOA, and PSO optimization algorithms to fine-tune the parameters to show the best transient performance can be achieved in SCiWOA optimal values of parameters as compared to WOA and PSO in the same SMIB power system.
- The SCiWOA optimized coordinated controller can be demonstrated under different input signals to the PSS and SSSC based lead-lag controllers of the same power system. It is observed from the demonstration that $\Delta\omega$ based input to PSS with $\Delta\omega$ based input to the lead-lag SSSC controller gives better transient performance as compared to $\Delta\omega$ based PSS with ΔP based input to the SSSC controller and ΔP based PSS with ΔP based input to the SSSC damping controller of the same SMIB power system.
- The coordinated control of SCiWOA optimized $\Delta\omega$based Type-2 FLC PSS with MLS input to Type-2 FLC SSSC controller is compared to $\Delta\omega$ based PSS with $\Delta\omega$ based SSSC and $\Delta\omega$ based PSS with MLS input to SSSC damping controller for testing the transient performance under different loading and fault conditions of the power system.
- The proposed controller can be applied further in three machine power systems for effectiveness and robustness of the transient stability analysis of the system. It is demonstrated in $\Delta\omega$ based input to a Type-2 FLC based PSS with MLS input to a Type-2 FLC lead-lag SSSC based damping controller under different types and locations of fault in the proposed system. It is overserved that Type-2 FLC coordinated control of SSSC controller gives better transient performance as compared to $\Delta\omega$ based input to PSS and MLS input to SSSC controller and $\Delta\omega$based input to PSS with $\Delta\omega$ based SSSC controller under three different contingencies of three machine power systems.

2. POWER SYSTEM MODEL

The proposed model comprises a 2100 MVA rated synchronous generator with a terminal voltage of 13.8 kV at 60 Hz connected to a long-distance double-circuit transmission line of 300km via a three-phase 13.8/500 kV step-up transformer and a 100 MVA SSSC FACTS controller installed as shown in Fig. 1. The 100MVA SSSC FACTS device, which is capable of injecting 20% of the system voltage, is connected in series with the transmission line between Bus 1 and Bus 2 to improve the power system stability. The generator is fitted with an excitation system, hydraulic turbine, and governor system [13, 27]. The various notations in Fig. 1, i.e., P_L, *I, VT,* V_B, V_{DC}, *and* V_{cnv}, are represented by line active power, current, generator terminal voltage, infinite bus voltage, input voltage to a voltage source converter (VSC), and output voltage of a VSC based SSSC controller, respectively.

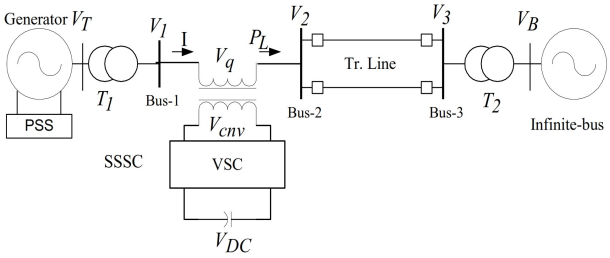

***Fig. 1**: Schematic of SMIB with SSSC and PSS.*

2.1 Overview of SSSC and Its Control System

The SSSC is a solid-state VSC based series compensator FACTS device that can inject voltage in quadrature with the line current of the transmission line. The main merit of the SSSC controller is that it controls the power flow of the transmission line because of its ability to offer inductive and capacitive operating modes. By changing the magnitude and polarity of the injected voltage, the compensation level can be dynamically controlled, and the system can be run in both capacitive and inductive modes. Fig. 2 shows a single-line block diagram of the SSSC control scheme. The SSSC controller injects a controllable AC voltage source into a power grid and is installed in series with power transmission lines. It is a voltage-sourced converter whose output is connected to the secondary side of the coupling transformer to regulate the injected voltage. To extract a voltage from a direct current (DC) power supply, the VSC used forced commutated control electronic devices. A DC voltage source is provided by a capacitor mounted to the VSC's DC side. To achieve the appropriate VSC pulses, the AC voltage regulator and DC voltage regulator are used. A limited amount of active power is taken from the line to hold the capacitor charged and to compensate for transformer and VSC losses. In this control system for SSSC, VSC with IGBT-based PWM inverters is used. The modulation index of the PWM modulator is adjusted to transfer the converter voltage.

As a result, the equations for power flow and transmission in the power system are as follows:

$$\mathrm{P}_q = \frac{V^2}{X_{eff}}\sin\delta = \frac{V^2}{X_L(1-\mathrm{X}_q/X_L)}\sin\delta \qquad (1)$$

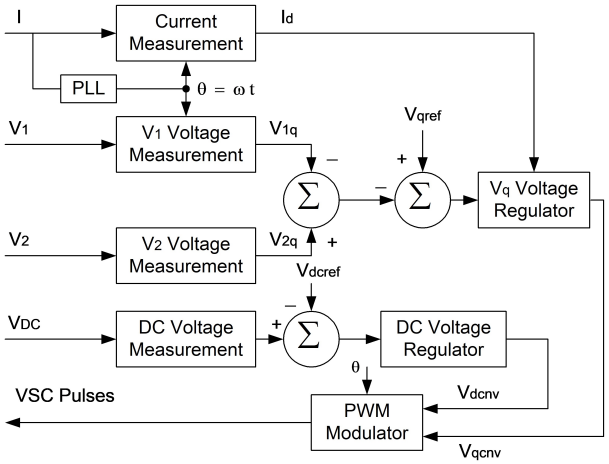

***Fig. 2**: Single-line block diagram of control system of SSSC.*

$$Q_q = \frac{V^2}{X_{eff}}(1-\cos\delta) = \frac{V^2}{X_L\left(1-\frac{X_q}{X_L}\right)}(1-\cos\delta) \quad (2)$$

where V, X_{eff}, and δ stand for bus voltage, effective reactance of the line, and power angle, respectively. The X_L and X_q represent the reactance of the transmission line and the SSSC compensating reactance, respectively. The control structure based on SSSC consists of the following: The direct-axis and quadrature-axis components of three-phase voltages and currents are computed using the output of a phase-locked loop (PLL) that synchronizes on the positive-sequence portion of the current I that can be found by the component of line current and voltage along the d-axis. All the instruments that are measured by measurement systems in the q components of voltages V1q and V2q as well as AC and DC voltage regulation. AC and DC voltage regulators determine the two components of the converter voltage (V_{dcnv} and V_{qcnv}).

3. THE PROPOSED COORDINATION DESIGN APPROACH

3.1 Type-2 Fuzzy Logic Overview

The traditional fuzzy logic control may not be effective for system performance due to more uncertainties. As per the literature, there are four processes of fuzzy logic control: fuzzification, knowledge base, interference, and defuzzification. Fuzzification is a process in which the input data is transformed into a linguistic variable. In this process, input data for the control variable, such as speed or power, is measured, and scaled values are transferred to the fuzzy variable with appropriate membership function values. A control rule set is created from knowledge-based data and includes the database with the necessary linguistic definitions. Inference mechanisms are developed through simulation work, which works under decision and control actions based on fuzzy logic. Fuzzy Inference System (FIS) is a process to interpret the values of the input vector and, on the basis of some sets of fuzzy rules, assign corresponding values to the output vector. This is a method to map an input to an output using fuzzy logic. Based on this mapping process, the system makes decisions and distinguishes patterns. Mamdani fuzzy inference is a set of linguistic control rules obtained from experienced human operators. In this method, the output of each rule is a fuzzy logic set.

Table 1 is the rule base of the fuzzy controller. In the defuzzification interface, the inferred linguistic variables are converted into a non-fuzzy control action of a numerical value for the plant input. The decision-making logic that creates a foundation for fuzzy logic action from the knowledge base, linguistic variables, and human decision-process to join together and provide the appropriate decisions Type 2 sets are used for modeling more uncertainty and impressions in a better way. The set theories are implemented in the fuzzy logic control rule of the IF-THEN statement for the design of fuzzy-based PSS in power systems. In this thesis, Mamdani-type fuzzy rules are used where the controlled output is fuzzy sets that need to be defuzzed to find a crisp value. The error signal of the plant is sensed by a fuzzy controller through a couple of scaling factors.

The membership functions having the shapes of trapezoidal, triangular, and bell-like structures are chosen because of their ease of functional illustration. Moreover, fuzzy inference engines may be used for the efficient manipulation of such functions, and due to their low usage of memory, they are very useful for acquiring the requirements of real-time applications. Out of all the membership functions, the triangular membership function is most accepted for real-time implementations of controller architecture as comparable to other alternatives because of its parameter-like functional representation. Considering the above points, in this present study, triangular MFs have been considered. In addition, similar MFs are also required for a good simulation setup, such as good memory utilization, computing efficiency, and performance analysis. For all inputs (error and error derivative) of the fuzzy system and FLC output, equivalent membership functions are then chosen. In this study, five fuzzy linguistic MFs variables are taken, which are shown in Table 1 for both inputs and outputs, and the Mamdani Fuzzy Interface System is considered.

Fig. 3 shows the MFs for input and output. In this regard, the error signal (e) and derivative error (de) are referred to as the two input signals of the FT2LL controller. As per the literature survey, double MF based type-2 fuzzy controllers provided the best performances in PSs. The proposed work considered a type-2 fuzzy logic control-based lead-lag controller structure for the improvement of stability analysis. The upper MF (UMF) and lower MF (LMF) are used in the MFs of type-2 fuzzy logic control, and the conjoining of UMF and LMF establishes a barrier. The development of a footprint of uncertainty (FOU) is constrained between UMF and LMF. Fuzzification, knowledge base, type reducer (TR), and

defuzzification are all part of type-2 fuzzy logic control. In FLC, the first stage is fuzzification, which processes the inputs and uses MFs to generate the desired structured fuzzy sets. The negative Big (NB), Negative Small (NS), Zero (Z), Positive Small (PS), and Positive Big (PB) are the linguistic variables used for membership functions. The type-2 fuzzy set (*FS*) can be represented as:

$$FS = \left((Var, a), \mu_U(Var, a)\right), vVar \in P, va \in J_{Var}[0,1] \tag{3}$$

where $\mu_U(Var, a)$is the UMF, *Var* is the main variable, *a* is the added variable of domain $\mathfrak{J}_{Var}$

The universe of discourse is expressed as:

$$FS = \int_{Var \in P} \int_{a \in J_{Var[0,1]}} \frac{\mu_E(Var, a)}{(Var, a)} \tag{4}$$

where, $\int \int$ = Union on *ACE* and *a*.

Now the equations can be written as:

$$\mu_{\underline{U}}(Var, a) = \overline{FOU(U)} vVar \in P, va \in J_{Var}[0,1] \tag{5}$$

where $\mathfrak{J}_{Var}$ is expressed as:

$$JVar = [\mu_{\overline{U}}(Var, a), \mu_{\underline{U}}(Var, a)] vVar \in P,$$

$$va \in J_{Var}[0,1] \tag{6}$$

The MF related to type-I FLC motivates us to cultivate LMF and UMF. The knowledge base includes a rule base and an interface engine. The rule base is demonstrated in Table 1. Individually *Var* and *dAVar* are the input signals to type-2 FLC, which generates output y.

The characteristic of the type-2 FLC is

$$LMF : forVar = \underline{LN}; dVar = \underline{Z}; Y = \underline{LN} \tag{7}$$

$$UMF : forVar = \overline{LN}; dVar = \overline{Z}; Y = \overline{LN} \tag{8}$$

The related FS firing forte is

$$\underline{f^s} = \min(\mu_{\overline{US}}(Var, a), \mu_{\overline{US}}(dVar, a)) \tag{9}$$

$$\overline{f^s} = \max(\mu_{\overline{US}}(Var, a), \mu_{\overline{US}}(dVar, a)) \tag{10}$$

$$F^S = [\underline{f^s}, \overline{f^s}] \tag{11}$$

TR is used to change type-2 to type-1 FS in order to defuzzify. The center of sums, centroid, and center of sets (SOC) are the approaches for defuzzification, with SOC being considered the best approach. The outputs are taken as:

$$Y_{\cos} = \sum_{s=1}^{25} \frac{F^s Y^s}{F^s} = [Y_{m1}, Y_{m2}] \tag{12}$$

$$Y_{m1} = \frac{\sum_{s=1}^{25} \underline{f^s} y^s}{\sum_{s=1}^{25} \overline{fy}} \tag{13}$$

$$Y_{m2} = \frac{\sum_{s=1}^{25} \overline{f^s y^s}}{\sum_{s=1}^{25} \overline{fs}} \tag{14}$$

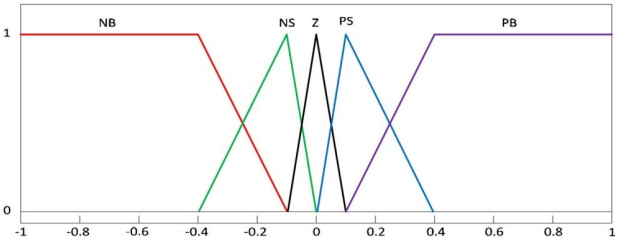

***Fig. 3**: MFs FLC inputs/output.*

***Table 1**: Rule base of fuzzy controller.*

e \ $\dot{e}$	NB	NS	Z	PS	PB
NB	NB	NB	NS	NS	Z
NS	NB	NS	NB	Z	PS
Z	NS	NS	Z	PS	PS
PS	NS	Z	PS	PS	PB
PB	Z	PS	PS	PB	PB

where Y_{m1} and Y_{m2} are related to two MF of type-1 FLC.

By averaging, type-2 FLC output is obtained. The suggested Type-2 lead lag controller is established, taking into consideration all lead lag controller and type-2 FLC characteristics.

3.2 Type-2 Fuzzy Logic Lead Lag Controller with Modified Local Input Signal

Fig. 4 shows the structure of a type-2 FLC based lead-lag SSSC damping controller. The proposed structure consists of a delay block, scaling factor blocks for fuzzy input (K_1 and K_2), a gain block (Ks), a signal washout block, and a two-stage phase compensation block. The phase compensation block is connected to compensate the SSSC-injected voltage V_q in order to compensate for the phase lag between input and output signals. The washout blocks function like a high pass filter with a time constant T_w, and the value will vary from 1 to 20 seconds. In this study, the washout time constant Tw = 10 seconds is used. The series injected voltage is modulated during the dynamic period to damp the system oscillation, which is represented by

$V_q = V_{qref} + \Delta V_q$, where $V_{qref}$is the injected voltage reference as required by the steady state power flow control loop, and ΔV_q is the change in injected voltages. ΔV_q and V_{qref} are stay constant during the steady state. Both local and remote signals are used as inputs to controllers, but for the effective design of the controller, a suitable choice of input signal is very important for correct control action during large disturbances. The most suitable choice of input signal is a local signal, as it is more reliable, cost-effective in terms of communication, and locally measurable, but its main disadvantage is that it cannot obtain the required oscillation modes. In wide-area signals, local signals are not highly controllable and observable. The remote signal is also not reliable as

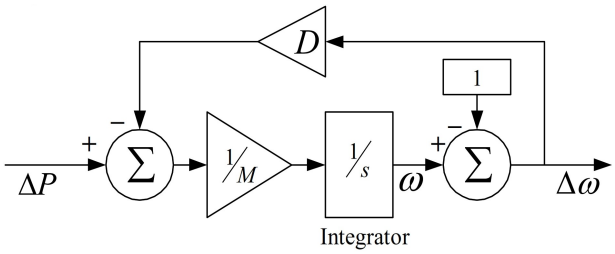

***Fig. 4**: Block diagram for representation for modified local input signal.*

compared to the local signal. So, the local signal can be modified to convert the remote signal. The speed deviation ($\Delta\omega$) is represented as a remote signal and the local power (ΔP) as a local signal. The speed of the generator and active power can be related as in Eq. (15).

$$\dot{\omega} = \left[P_m - P_e - D(\omega - 1)\right] / M \tag{15}$$

Where, P_m is input power of the synchronous generator.
P_e is the output of the synchronous generator
M is the inertia constant
D is the damping coefficient
The speed of the rotor can be express in equation (16)

$$\Delta\omega = \int \left([\Delta P - D(\omega - 1)] / M\right) \tag{16}$$

The equation (16) can be represented in the form of a block diagram, which is shown in Fig. 4.

The fall detection system for patients or the elderly involves installing a device on the person. As the person moves, the device collects X, Y, and Z axis values. These values are then analyzed to determine if the person has experienced any of the four types of falls according to the predefined schedule.

Once the values are analyzed, in the event of an actual fall, the data is sent from the NB-IoT device to the UDP Server and Application Server. The data is stored in the database, allowing it to be displayed on web applications for further reference. Additionally, an alert is sent to the Line application to notify individuals involved with the patient or elderly person, enabling them to provide immediate assistance, as shown in Fig. 4 [16].

In NB-IoT (Narrowband Internet of Things), UDP is one of the transport layer protocols. That is supported for sending data between devices and servers. Because NB-IoT is designed for low-power and low-bandwidth devices, UDP is therefore a good choice for sending small amounts of data quickly and efficiently. However, because UDP has no reliability or error detection, applications that use it must therefore be designed to handle packet loss or corruption.

The nature of data transmission between NB-IoT devices and UDP servers is ideal for NB-IoT devices with low bandwidth and low power consumption with low latency. It is designed for the transmission of small, modular data and data packets.

3.3 Type-2 FLC of Power System Stabilizer (T2FLC PSS)

The Type-2 FLC based power system stabilizer structure is shown in Fig. 6. It is primarily used to apply damping to the oscillations of the generator rotor by using the auxiliary stabilizing signal to control its excitation. It consists of a lead-lag compensation block, a signal washout block, a proportional and integral gain block, and a sensor delay block of the T2FLC PSS structure. The additional excitation voltage is calculated using the speed deviation as an input to the T2FLC PSS. The proposed SCiWOA optimization algorithm is employed to find out the tuning parameters gain (Kp), scaling factors (K1 and K2), and time constants of the T2FLC PSS structure with the assumption of the washout time constant T_w=10[16]. The active power or remote speed deviation can be considered the input to the T2FLC PSS, and the output is voltage V_S which supports the extra input to the excitation system.

3.4 The proposed controller design based SCiWOA:

The coordinated control of $\Delta\omega$ based T2FLC PSS and MLS based T2FLC lead-lag-based SSSC controllers for the proper tuning parameters of the controller is used for transient stability improvement in SMIB power system.

In the design of a SCiWOA optimization technique-based controller, the objective function is first defined on the basis of the type of constraints. In the SMIB power system, the objective function is the speed deviation of the synchronous generator. The proposed work, the integral time multiplied absolute value of error, is used in the PSS with lead lag SSSC controller and the T2FLC PSS with T2FLC lead lag SSSC controller to demonstrate the transient performance of the power system and can be written as certain constraints, which can be expressed as an optimization problem as follows:

Objective Function (ITAE=$\mathcal{J}$):

$$J = \int_0^{t_{sim}} |\ \Delta\omega\ | \cdot t \cdot dt \tag{17}$$

The tuning parameters of SMIB power system: K_1, K_2, K_S, K_P, T_{2S}, T_{3S}, T_{4S}, T_{1P}, T_{2P}, T_{3P}, T_{4P} Subjected to: ${K_1}^{\min} \le K_1 \le {K_1}^{\max}$,${K_2}^{\min} \le K_2 \le {K_2}^{\max}$(Scale factor)

$${K_S}^{\min} \le K_S \le {K_S}^{\max}, {K_P}^{\min} \le K_P \le {K_P}^{\max}$$

$${T_{1S}}^{\min} \le T_{1S} \le {T_{1S}}^{\max}, {T_{1P}}^{\min} \le T_{1P} \le {T_{1P}}^{\max}$$

$${T_{2S}}^{\min} \le T_{2S} \le {T_{2S}}^{\max}, {T_{2P}}^{\min} \le T_{2P} \le {T_{2P}}^{\max}$$

$${T_{3S}}^{\min} \le T_{3S} \le {T_{3S}}^{\max}, {T_{3P}}^{\min} \le T_{3P} \le {T_{3P}}^{\max}$$

$${T_{4S}}^{\min} \le T_{4S} \le {T_{4S}}^{\max}, {T_{4P}}^{\min} \le T_{4P} \le {T_{4P}}^{\max}$$

The SCiWOA optimization algorithm is employed to find the coordinated controller parameters of optimal value under the boundary between the minimum and maximum constraint values.

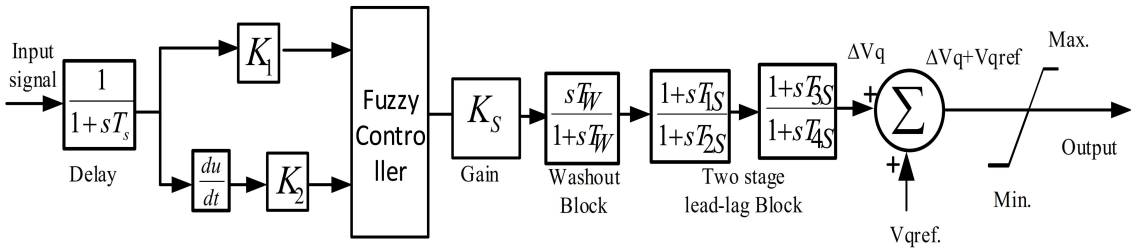

***Fig. 5**: The proposed Type-2 FLC LL SSSC controller structure.*

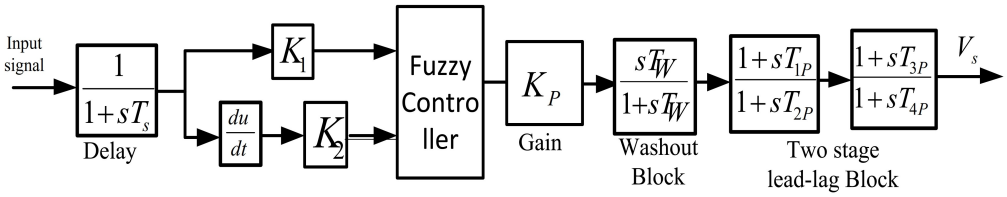

***Fig. 6**: Type-2 FLC PSS structure.*

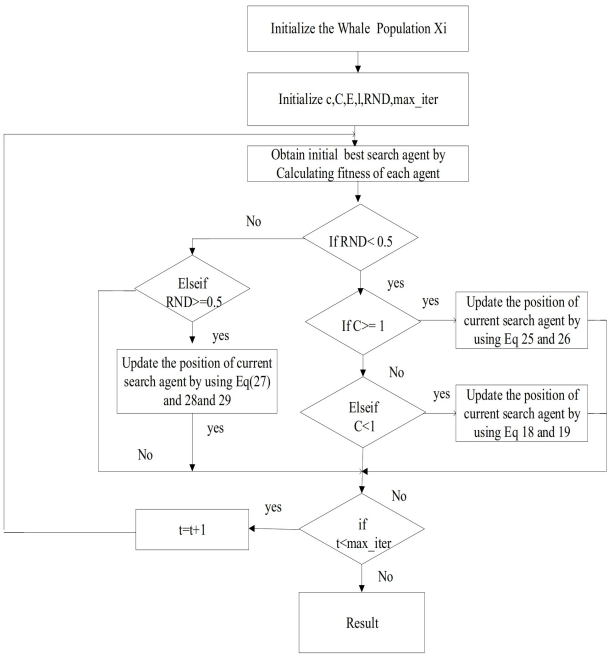

***Fig. 7**: Flow chart of SCiWOA optimization algorithm.*

4. OVERVIEW OF SINE COSINE ADAPTED IMPROVED WOA

The whale optimization process is established on humpback whales for the probing of food or prey [23–25]. Whales like to hunt their prey close to the water surface. This action of confronting is ruled by making bubbles in a circular route. To kill the prey, whales practice the system of swimming about the prey in a shrinking loop. As the position of the best pattern is unknown initially, the whales assume that the current finest candidate is close to the best. The remaining whales attempt to adjust their positions, guided by the best positions of the whales. In order to model mathematically in WOA the bubble-net attacking nature of whales Shrinking, encircling, and spiral updating position methods are approaches for the design. These two methods are described in the equation (18) - (20).

$$\vec{F} = \left| \vec{E}.\vec{Z}*(t) - \vec{Z}(t) \right| \tag{18}$$

$$\vec{Z}(t+1) = \vec{Z}*(t) - \vec{C}.\vec{F} \tag{19}$$

$$\vec{Z}(t+1) = \vec{F}'.e^{kl}.\cos(2\pi l) + \vec{Z}*(t) \tag{20}$$

$\vec{Z}(t)$ signify as the position vector, $\vec{Z}*(t)$ signify the best solution arrived at so far, t is representing the current iteration taking place, the vector coefficient $\vec{C}$and $\vec{E}$ can help for searching areas to find out the whale in proximate proximity of prey. The equation (18) guarantees that any whale will revise its location in the vicinity of the current best whale. It is ensuring that any search particle will update the position in the vicinity of the current best solution in the equation (19). In the equation (3) $\vec{F}' = \left| \vec{Z}*(t) - \vec{Z}(t) \right|$ is the distance from the i^{th} whale to the finest found prey till now, *l'* which represents an arbitrary number that varies in the interval [-1, 1], and '*k*' is specified as the contour of the logarithmic spiral.

The vector coefficients$\vec{C}$and $\vec{E}$are evaluated from the equations (21) and (22) given as

$$\vec{C} = 2\vec{c}\,\vec{r} - \vec{c} \tag{21}$$

$$\vec{E} = 2\vec{r} \tag{22}$$

In the equations (21) and (22),$\vec{r}$ is an arbitrary number chosen between range 1 and 0. The $\vec{c}$reduces from 2 to 0 linearly in the optimization process. The shrinking

nature of $\vec{c}$ reduces the guaranteed value. The equation (23) $\vec{c}$ is defined as the distance control parameters decreasing linearly during both exploration and exploitation phases, given as

$$\vec{c} = 2 - t\frac{2}{ITER_{MAX}} \tag{23}$$

Whereas 't is representing the current iteration $ITER_{MAX}$ is the maximum iteration in the search process. The anticipated SCiWOA uses a sine function for the control parameter '$\vec{c}$'in the process as equation (24).

$$\vec{c} = \begin{cases} 1 - \sin\left(\frac{\pi}{2}(\frac{t}{ITER_{MAX}})\right) & if\ RND < 0.5 \\ 1 - \cos\left(\frac{\pi}{2}(\frac{t}{ITER_{MAX}})\right) & if\ RND \geq 0.5 \end{cases} \tag{24}$$

Where the range of the arbitrary *RND* value varies between 0 to 1. The incorporation of exploration and exploitation fluctuating during the total iteration process takes place by using the sine and cosine functions $\vec{c}$ in the equation (24). The cyclic decays of the sine and cosine functions permitted an agent in the search process to be repositioned around an extra new agent [26]. This process can guarantee the exploitation and exploration of the search space defined between the solutions. In the WOA, the target whales are the best whales, and all other whales aim to update their positions near the best whale. In the early stages, the most likely search agent is unknown. Therefore, this method of modifying involves employing huge steps at the beginning, which may result in moving the whales toward the distant optimal value. Consequently, the institution of scaling factors (SF) in SCiWOA regulates the upgrading of the movement of search agents during the search process and is related to equations 25–27 as given below:

$$\vec{F} = \left|\vec{E}.\vec{Z}*(t) - \vec{Z}(t)\right|/SF \tag{25}$$

$$\vec{Z}(t+1) = (\vec{Z}*(t) - \vec{C}.\vec{F})/SF \tag{26}$$

$$\vec{Z}(t+1) = (\vec{F}'.e^{kl}.\cos(2\pi l) + \vec{Z}*(t))/SF \tag{27}$$

In the exploration phases, which incorporate the scaling factor in the search processes. In the WOA, search agents upgrade their positions in each iteration in accordance with the randomly selected agent in the exploration phase. It should cause random changes in whales' movements in the preliminary phases of the search process. Therefore, in the present SCiWOA technique, the position of search agents is changed by scaling factors, as in equations (28) and (29)

$$\vec{F} = (\vec{E}.\vec{Z}_{rand}(t) - \vec{Z})/SF \tag{28}$$

$$\vec{Z}(t+1) = (\vec{Z}_{rand} - \vec{C}.\vec{F})/SF \tag{29}$$

The *SF* is varying which represented as in equation (30) of equation 28 and 29

$$SF = \begin{cases} 2 - \frac{t}{ITER_{MAX}} & if\ RND1 < 0.5 \\ 1/(2 - \frac{t}{ITER_{MAX}}) & if\ RND1 \geq 0.5 \end{cases} \tag{30}$$

Where *RND*1 is a range of random values in the interval chosen between 0 and 1. The scaling factors are combined in both phases to change the movement of whales throughout the beginning stages of the search process for refining the search capability. The best value is attained in the later stages of the search process, subjected to the normal movement of whales in the process. The flow chart for the proposed SCiWOA algorithm, which is shown in Fig. 7.

5. RESULTS AND DISCUSSIONS

The simulation results of the system are carried out in MATLAB by employing the Simulink test model of the SMIB power system considered. Moreover, the SCiWOA code is implemented in a.m file and interfaces with the Simulink test model of a power system by using the SimPowerSystems toolbox to carry out the optimization process. The dynamic simulation results are performed with a 64-bit, 2.7 GHz Intel Core i5 CPU on a system. The objective function ITAE can be calculated under a three-phase fault disturbance that is considered in one of the parallel transmission lines in the SMIB power system. The optimization algorithms of PSO, WOA, and SCiWOA are initially set with parameters before running the simulation model of the power system. The initial parameters of the PSO algorithm (maximum generation 200, swarm size 40, cognitive and social constants (c1 = c2 = 2 and inertia weight (wmax = 0.9 and wmin = 0.2). The WOA and SCiWOA optimization algorithms initial setting parameters (number of solutions = 40, number of generations = 200, c [0 2], linear decrease coefficient, l [-1 1] random value, k = 1) are considered for the optimization problem in the proposed power system. The optimization is repeated at least 20 times in the simulation model of coordinated control of $\Delta\omega$based PSS with MLS input to a lead-lag-based SSSC controller in a SMIB power system, and the best final value of the tuning parameter is considered as in Table 2. In the same procedure, the optimal controller parameters are obtained by using PSO and WOA optimized in the same controller and in the same structure of the power system, as shown in Table 2. The number of generations and the number of populations are considered the same in all the three-optimization techniques for finding out the optimal parameters of the same power system. Table 2 shows the minimum fitness values along with the maximum and average fitness values obtained by 20 time runs of the optimization algorithm. It is clear from Table-2 that the minimum values of ITAE obtained with SCiWOA, WOA, and PSO in coordinated control of PSS with a modified local signal input-based lead lag SSSC controller are 4.8361×10^{-4}, 6.8924×10^{-4}, 7.3175×10^{-4}

***Table 2**: The Optimal parameters of the coordinated control of $\Delta\omega$ based PSS and MLS input to SSSC controller.*

Input Signal/ Parameters		Techniques with ITAE Objective function					
MLS input to LL based SSSC controller with		SCiWOA		WOA		PSO	
$\Delta\omega$ based input to PSS		SSSC	PSS	SSSC	PSS	SSSC	PSS
K_S/K_P		59.7494	17.9810	8.3121	2.3170	3.0011	0.7917
T_{1S}/T_{1P}		0.8389	1.3962	2.3059	2.0521	2.0340	0.1563
T_{2S}/T_{2P}		0.7478	1.8566	0.8182	2.3798	0.1927	1.7549
T_{3S}/T_{3P}		1.1321	1.0614	2.0104	0.1916	0.8868	0.2171
T_{4S}/T_{4P}		1.0572	1.0740	1.3461	1.7720	0.3309	1.5424
ITAE	Minimum	4.8361×10^{-4}		6.8924×10^{-4}		7.3175×10^{-4}	
	Average	$5.3901 \times 10{-}4$		7.1140×10^{-4}		8.6411×10^{-4}	
	Maximum	6.1268×10^{-4}		7.2104×10^{-4}		9.4383×10^{-4}	

***Table 3**: The Optimal parameters of the coordinated control under different input signal of PSS and SSSC controller using SCiWOA optimization Techniques.*

Input Signal/Parameters		Ks/Kpss	T1s/T1p	T2s/T2p	T3s/T3p	T4s/T4p	ITAE
$\Delta\omega$ based LL controller with	SSSC	58.6444	1.6881	0.9032	1.5511	2.0281	5.8821×10^{-4}
$\Delta\omega$ based PSS (Case-A)	PSS	0.9639	0.2106	2.4370	1.6287	0.5789	
ΔPa based LL controller with	SSSC	4.8528	2.0957	0.3535	1.8308	1.7280	6.5303×10^{-3}
$\Delta\omega$ based PSS (Case-B)	PSS	0.1734	1.2227	2.4285	0.2820	1.8583	
ΔPa based LL controller with	SSSC	1.8781	2.0388	0.0044	0.0087	0.2196	7.3369×10^{-3}
ΔPa based PSS (Case-C)	PSS	13.0371	0.0489	1.0608	0.8533	1.3538	

respectively. From the table, it is clear that SCiWOA algorithm-based coordinated controllers in SMIB power systems have a percentage reduction in ITAE value compared to WOA and PSO optimization techniques of 29.83% and 33.91% respectively. It is observed that the proposed SCiWOA based IATE algorithm best values as dominance over WOA and PSO algorithms for the same power system model. It is also observed that, as per Table 3, the ITAE values under Cases A, B, and C are 5.8821×10^{-4}, 6.5303×10^{-3} and 7.3369×10^{-3} respectively. From Table-2 and Table-3, it is clear that SCiWOA optimized coordinated control of MLS based SSSC based LL controllers with $\Delta\omega$ based PSS also ITAE value dominance over the Case-A (12.75%), Case-B (21.435%), and Case-C (93%) percentage of reduction of ITAE value. However, in the proposed coordinated control of a T2 fuzzy lead-lag SSSC based controller with T2 fuzzy PSS for the tuning parameters, the ITAE value 3.1694×10^{-4} is obtained in the same power system as per Table 3. It is observed that with the proposed SCiWOA optimized T2Fuzzy SSSC based coordinated controller, there is a reduction of ITAE value is 38.41% as compared to the same optimized MLS input SSSC based LL controller with a power system stabilizer of the same power system. To demonstrate the effectiveness and robustness of the analysis of the coordinated controller of PSS with SSSC controller under three optimization techniques as in Table 2, and different types of input signal of PSS and SSSC as in Table 3, can be analysed in three loading conditions (nominal loading, light loading, and heavy loading) are considered. The simulation model of the power system is carried out with different transient disturbances and fault clearing sequences to analyze the transient stability of the proposed power system. The response of SCiWOA optimized coordinated control of MLS input to LL based SSSC damping controller with $\Delta\omega$based input to PSS is shown as a solid line with a legend (SCiWOA:MLS-SSSC+R-PSS The response of WOA-optimized coordinated control of MLS input to LL based SSSC damping controller with $\Delta\omega$ input-based PSS is shown as a dashed dash line with a legend.

WOA: MLS-SSSC+R-PSS. The response of PSO optimized coordinated control of MLS input to LL based SSSC damping controller with $\Delta\omega$ input-based PSS is shown as dotted line with legend PSO: MLS-SSSC+R-PSS.

Case I: Simulation result under Nominal Loading *($P_e = 0.75pu$,* Q_0= -0.0718 pu, $\delta_0 = 45.4^\circ$*)*

On the transmission line between Bus-2 and Bus-3, a 3-phase fault is applied in the middle of one line for time t = 1 sec, and the fault is restored after 3 cycles after it is cleared by tripping the faulted line of the system. The system response presented under this case I is shown in Figs. 8-10. Figure 6 shows the speed deviation response, and it is clear that coordinated control of SCiWOA optimized based damping controller transient response (SCiWOA: MLS-SSSC+R-PSS) is better as compared with WOA optimized remote input-based PSS and MLS input lead lag SSSC coordinated control (WOA: MLS-SSSC+R-PSS) and PSO optimized remote input PSS and MLS input SSSC controller (PSO: MLS-SSSC+R-PSS) of the same power system. It is also demonstrated under three loading conditions with different input signals taken as per Table 3 of the coordinated control of PSS with the SSSC damping controller in the proposed SMIB power

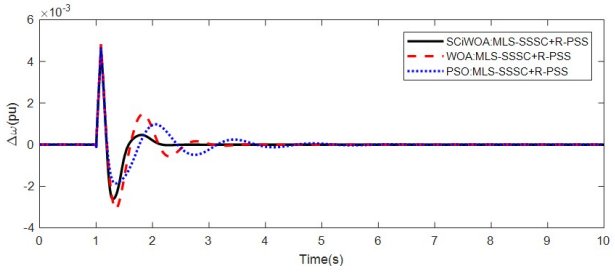

***Fig. 8**: Speed deviation response under SCiWOA, WOA and PSO based MLS input signal based SSSC with Δω based PSS.*

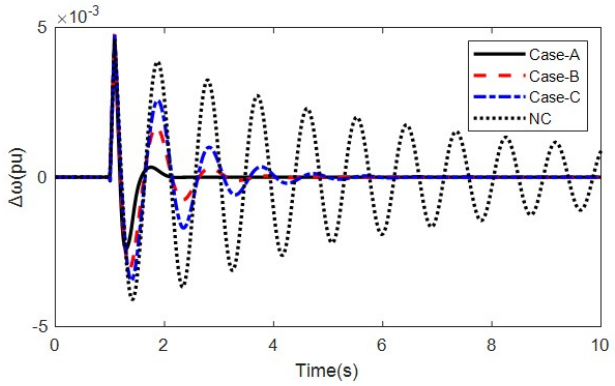

***Fig. 9**: Speed deviation response under case-1.*

system. The responses of speed deviation and power angle under this Case-I, as shown in Fig. 7-8, SCiWOA optimized $\Delta\omega$ based LL SSSC controller with $\Delta\omega$ based PSS coordinated control tuning parameters (Case-A) has superior performance as compared with ΔPa based LL controller with $\Delta\omega$ based PSS (Case-B) and ΔPa based LL controller with ΔPa based PSS (Case-C) of the same SMIB power system.

Case-II: Light Loading *($P_e = 0.4pu$, Q_0 =-0.1483pu,$\delta_0 = 29.46^0$)*

By applying the 3-phase fault adjacent to Bus-3 of the system at time t = 1 sec, the generator loading is changed to light loading as per Case-II to test the robustness analysis of the coordinated controller of the system. The original system is restored after three cycles of faulted lines have been cleared. The responses of the system under this condition are shown in Figs. 11-13, which demonstrate the coordinated controller's response to changes in operating conditions and fault location. Fig. 11 shows that the proposed approach of SCiWOA optimized coordinated control $\Delta\omega$ based PSS with MLS input based SSSC lead lag controller provides a superior transient response as compared to those WOA and PSO optimized coordinated controllers of the power system. It is also tested under light loading conditions for different optimization parameters as per Table 3 of the SMIB power system and system responses as shown in Figs. 14–15. It is clear that system responses of speed deviation as shown in Fig. 14 under no controller are highly oscillatory, and in the proposed SCiWOA

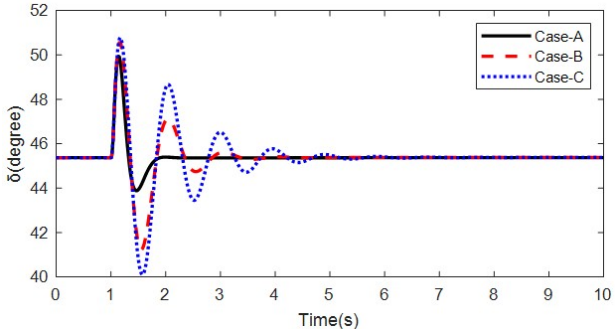

***Fig. 10**: Power angle deviation response under case-1.*

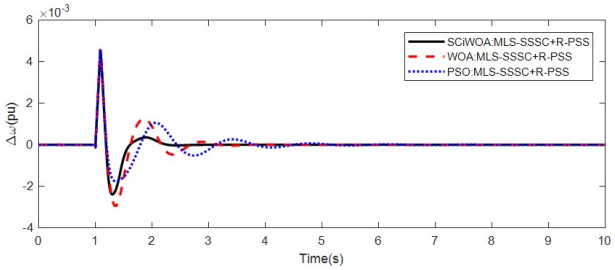

***Fig. 11**: Speed deviation response under SCiWOA, WOA and PSO based MLS input signal based SSSC with Δωbased PSS.*

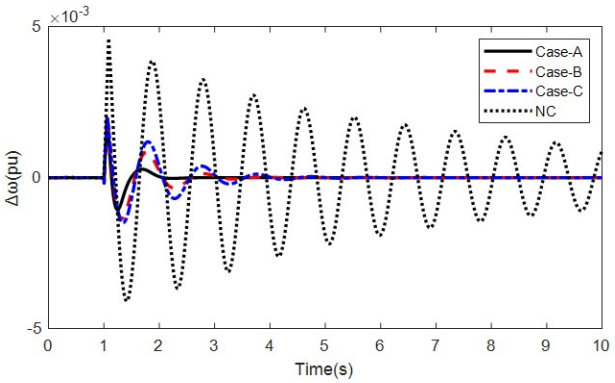

***Fig. 12**: Speed deviation response under Case-II.*

design, a coordinated control $\Delta\omega$ based PSS with $\Delta\omega$ based SSSC controller as in Case-A has superior transient performance as compared to Case-B and Case-C in terms of settling time and overshoot of the same power system.

Case-III: Heavy Loading *($P_e = 1.0pu$, Q_0= 0.05801pu ,$\delta_0 = 60.72^0$)* The effectiveness of the proposed coordinator controller is also demonstrated under heavy loading conditions by disconnecting the load at Bus-1 at time t = 1 s for 100 ms. Figs. 14–16 show the system responses for the above contingency. It is clearly seen that the power system oscillation was dampened effectively and became stable very quickly in SCiWOA optimized coordinated control of tuning parameters as compared to WOA and PSO optimized tuning parameters of the same controller and structure of the power system.

It is also tested under different input signals to the PSS

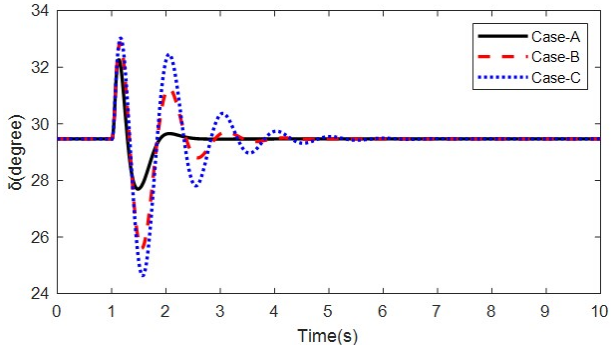

***Fig. 13**: Power angle deviation response under Case-II.*

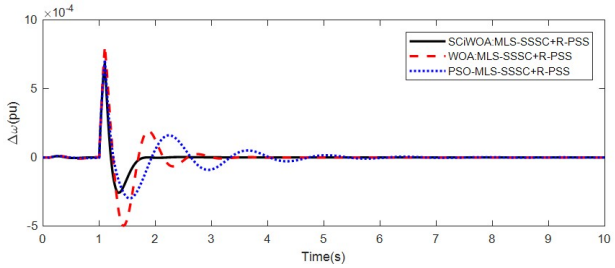

***Fig. 14**: Speed deviation response under SCiWOA, WOA and PSO based MLS input signal to SSSC with $\Delta\omega$ based PSS.*

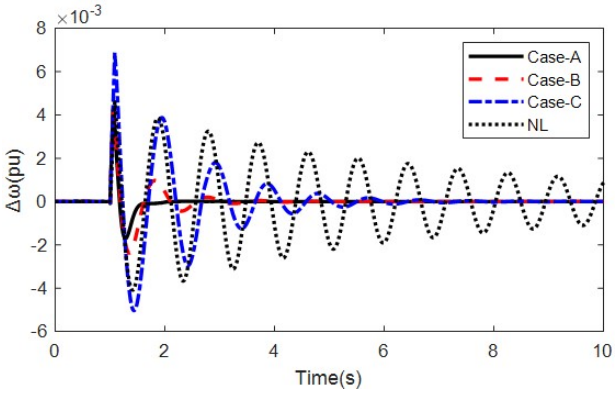

***Fig. 15**: Speed deviation response under Case-III.*

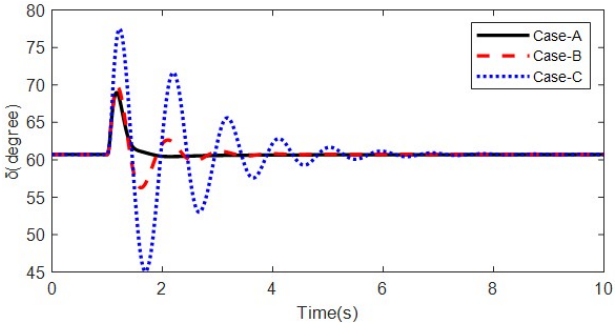

***Fig. 16**: Power angle deviation response under Case-III.*

and SSSC controllers as per Table 3. Under this loading condition, it shows responses as in Figs. 13–14, and it is observed that SCiWOA optimized coordinated control as in Case-A has better transient performance as compared to Case-B and Case-C of the same power system.

From the above analysis of Case-I, Case-II, and Case-III, it is observed that SCiWOA optimized coordinated control using MLS input-based SSSC damping controller with $\Delta\omega$based power system stabilizer gives better transient performance as compared to WOA and PSO based coordinated control of the same power system. It is also observed that SCiWOA optimized $\Delta\omega$ based PSS with $\Delta\omega$ based SSSC controller superior transient performance as compared to $\Delta\omega$ based PSS with ΔPa based LLSSSC controller and ΔPa based PSS with ΔPa based SSSC controller, respectively, in terms of settling time and overshoot of the SMIB power system. However, from the analysis, it is clear that coordinated control of MLS input to the SSSC based lead lag controller with $\Delta\omega$ based PSS gives better choice for the transient stability analysis of power systems.

5.1 Remote speed deviation ($\Delta\omega$) based input toType-2 PSS and MLS input-based Type-2 Fuzzy lead lag SSSC damping controller

In the same procedure as the previous analysis, optimal parameters are obtained using the SCiWOA optimization technique for the coordinated control of $\Delta\omega$ based input to the Type-2 FLC PSS with Type-2 FLC LL based SSSC damping controller parameter and conventional PSS with PI-based SSSC controller in SMIB power system. The optimal tuning parameters of the proposed coordinated controller are given in Table 4. A comparison between the coordinated control of SciWOA optimized design of MLS input-based PSS with SSSC lead lag controller (as in Table 2) ,coordinated control of $\Delta\omega$ based LL controller with $\Delta\omega$ based PSS (as in Table 3 of the best transient stability improvement of SSSC coordinated controller), and proposed coordinated control of Type-2 FLC PSS and Type-2 FLC lead lag SSSC based damping controller and conventional based PSS with PI type lead lag SSSC controller performances based on the transient stability improvement under three types of loading conditions with different faults is applied in different locations of the SMIB power system. The transient stability performance analysis can be demonstrated under three loading conditions (condition 1, condition 2, and condition 3) of the proposed SMIB power system.

Condition-1: (Nominal loading, Pe = 0.75 pu, Q_0= -0.0718 pu, $\delta 0$ = 45.4^0, fault is same as in case-I)

Condition-2:(Light Loading, $P_e = 0.5pu$, Q_0 *=-0.1483pu,*$\delta_0 = 29.46^0$, fault is same as in case-II)

Condition-3:(Heavy Loading, Pe=1.0 pu, Q_0*=0.05801pu,*$\delta_0 = 60.72^0$, fault is same as in case-III)

The system responses with SCiWOA optimized $\Delta\omega$ based input signal PSS with$\Delta\omega$ based SSSC PI controller are shown as a dotted line with the legend Case-1. The response with the proposed SCiWOA optimized $\Delta\omega$ based input signal PSS with$\Delta\omega$ based SSSC lead lag

***Table 4**: SCiWOA based optimal control parameters of the proposed coordinated controller.*

Input Signal/Parameters		KS/KP	T1S/T1P	T2S/T2P	T3S/T3P	T4S/T4P	K1S/K1P	K2S/K2P
MLS based Type-2 FLC in SSSC with LL		141.7438	0.2848	2.2823	1.2047	2.1297	99.2929	16.2560
$\Delta\omega$ based Type-2 FLC with PSS		161.9847	0.4677	0.6188	0.1364	1.5228	34.2507	14.4521
ITAE	Minimum	3.1694×10-4)						
	Average	3.8462×10-4						
	Maximum	4.0117×10-4						
SCiWOA optimized design of Conventional PSS with SSSC based PI Controller								
Input Signal/ Parameters		Ks				Kp		
SSSC based PI controller		70.4050				0.8852		
$\Delta\omega$ based PSS		Kp	T1p	T2p	T3p		T4p	
		0.9799	0.8278	1.0613	0.6764		0.4934	

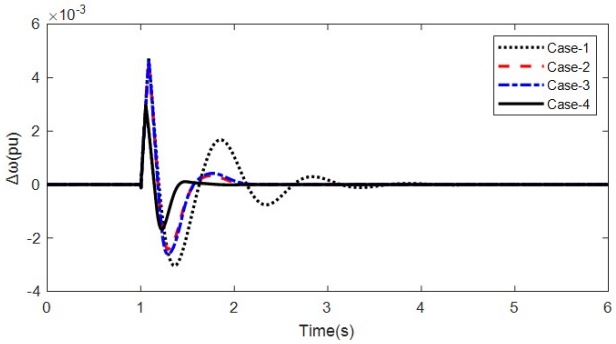

***Fig. 17**: Speed deviation response under Condition-1.*

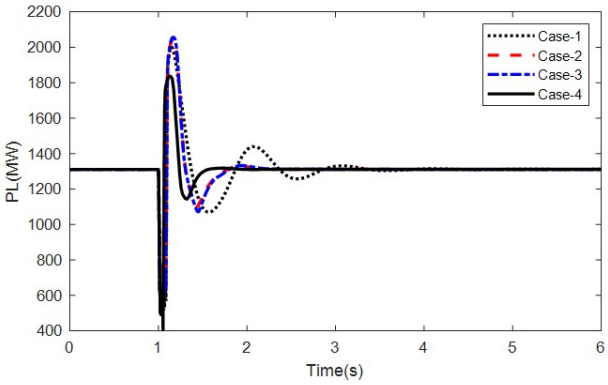

***Fig. 18**: Active power deviation response under Condition-1.*

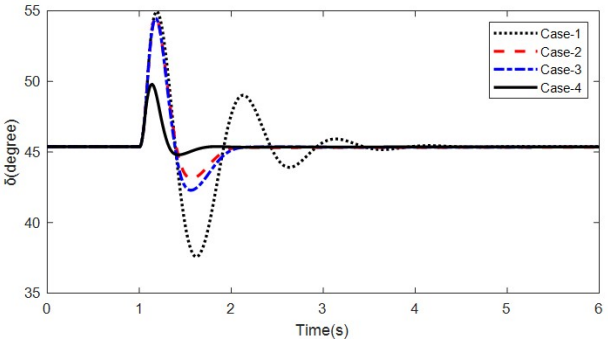

***Fig. 19**: Power angle deviation under condition-1.*

controller is shown dashed line with a legend. Case-2. The response with the proposed SCiWOA optimized $\Delta\omega$ input-based PSS with MLS based lead-lag SSSC damping controller is shown as a dashed dot line with the legend Case-3. The response with the proposed SCiWOA optimized $\Delta\omega$ input signal-based Type-2 fuzzy PSS and MLS based Type-2 fuzzy lead-lag SSSC damping controller is shown as a solid line with the legend Case-4. The system responses of speed, line active power, power angle, and output voltage of the Type-2 FLC lead lag controller of the power system under condition 1 are shown in Figs. 17–19. It is clear that SCiWOA optimized MLS input signal-based Type-2 Fuzzy PSS with MLS based Type-2 Fuzzy lead lag SSSC damping controller (Case-4) has superior transient performance as compared to Case-1, Case-2, and Case-3. However, the transient stability performances of cases 2 and 3 are better as compared to cases 1 of conventional PSS with PI controllers of the same power system. Fig. 20 shows the responses of the output voltage of the T2Fuzzy Power system stabilizer under nominal conditions, which improve transient performances as compared to Case-1, Case-2 and Case-3 of the system.

5.2 Multi-machine power system with SSSC

Now, to check the effectiveness of the analysis of transient improvement, it is further extended to a multi-machine power system. A three-machine bus power system, as shown in Fig. 27, which can be demonstrated for coordinated control of $\Delta\omega$ based T2FLC PSS's with MLS input-based T2FLC lead-lag SSSC damping controllers. The proposed system is made up of three generators that are split into two areas and linked by a tie-line. Two 2100MVA/13.8KV generator units are installed in one part of the area, and one 2400MVA/13.8KV generator is installed in another part of the area [28–30]. The line is sectionalized to improve power system reliability, and SSSC is installed in the middle of the tie line between two regions. Each synchronous generator has a T2FLC based PSS connected to the excitation system of the generator. The simulation of the proposed power system model can be developed by using the parameters as per

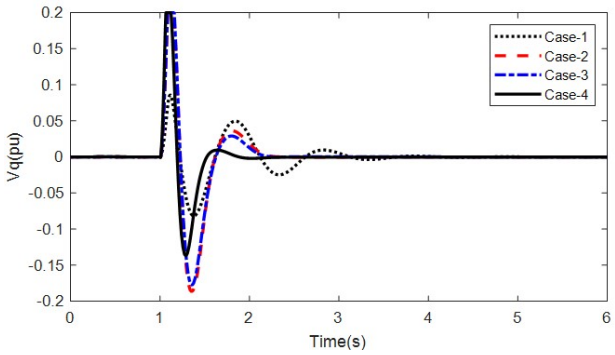

***Fig. 20**: Output voltage of T2Fuzzy PSS under condtion-1.*

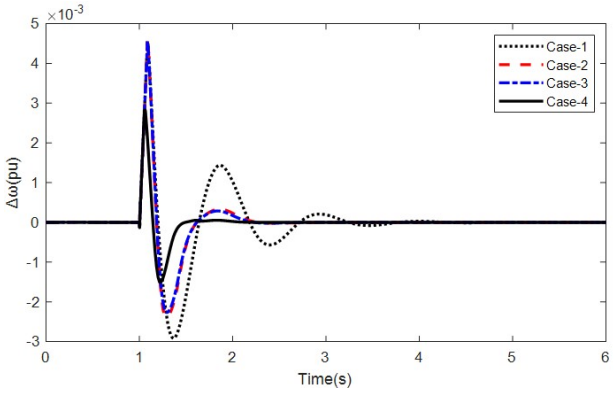

***Fig. 21**: Speed deviation under condition-2.*

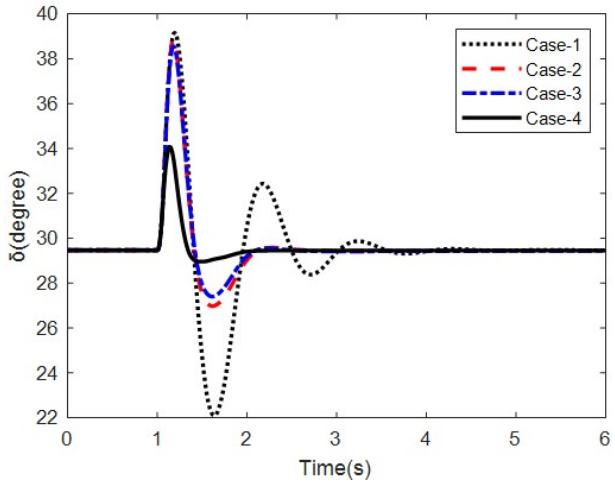

***Fig. 22**: Power angle response under condtion-2.*

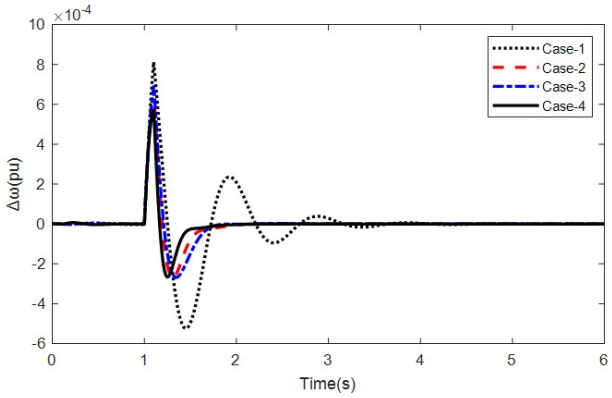

***Fig. 23**: Speed deviation under condtion-3.*

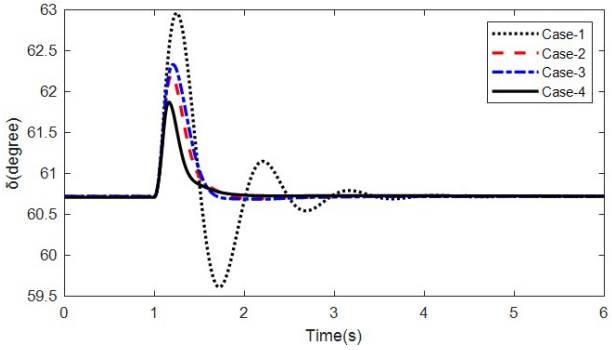

***Fig. 24**: Power angle response under condtion-3.*

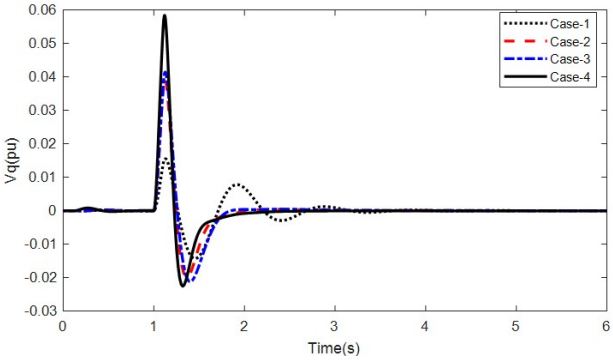

***Fig. 25**: Output of T2Fuzzy LL SSSC controller under condition-3.*

the appendix. The objective function J can be defined by the sum of speed deviations between inter-area and local modes of oscillation of the three machines (G1, G2, and G3) in the power system. In the proposed analysis, speed devotion $\Delta\omega_I$ between the generators remote G1 and G2 is the inter-area mode, and speed deviation $\Delta\omega_L$ between generators G2 and G3 is the local mode of oscillation. The real active power measured nearest to Bus-3 is considered a local signal. The ITAE objective functions (J) are defined in the three-machine 6-bus system as given:

$$J = \int_{t=0}^{t=t_{sim}} \left(\sum |\Delta\omega_L| + \sum |\Delta\omega_I|\right) \cdot t \cdot dt \qquad (31)$$

Where t_{sim} is the time range of the simulation. The same procedure as discussed in the SMIB power system can be used to determine the optimal value of coordinated controller parameters in three machine power systems. The best optimal value of tuning controller parameters is obtained, as shown in Table 6, for three different approaches to coordinated control of the proposed power system. The objective function values and controller parameters are obtained by employing the SCiWOA optimization algorithm in three cases of coordinated

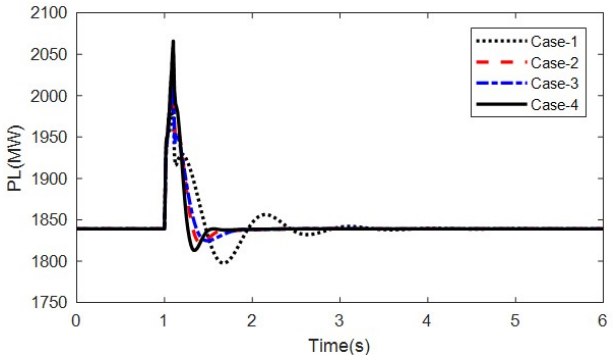

***Fig. 26**: Line active response under condition-3.*

***Table 5**: The performance of speed deviation under different loading condition.*

Loading condition	Input Signal/ Parameters	Overshoots in $\Delta\omega$ ($\times10^{-3}$)	Undershoots in $\Delta\omega$ ($\times10^{-3}$)	Settling Time
Nominal Loading	Case-1	4.8011	-3.7852	4.5661
	Case-2	4.7810	-3.4106	1.7447
	Case-3	4.7417	-2;6918	1.4521
	Case-4	2.9732	-1.9301	1.1315
Light Loading	Case-1	4.7893	-3.1056	4.3411
	Case-2	4.7581	-2.8014	1.8836
	Case-3	4.7471	-2.5496	1.6734
	Case-4	2.8405	-1.8392	0.9984
Heavy Loading	Case-1	8.2574	-5.8743	4.6733
	Case-2	7.2775	-3.2472	2.3605
	Case-3	7.2381	-2.9142	1.1472
	Case-4	5.8163	-2.6720	0.7841

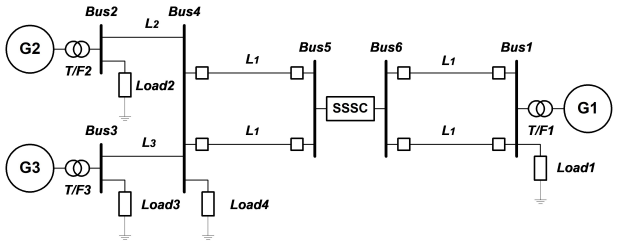

***Fig. 27**: Implementation of SSSC in 3 machine power system.*

controllers of power systems, as shown in Table 6. It is clear from Table 6 that the ITAE value in the proposed coordinated control of SCiWOA optimized $\Delta\omega$ based input to T2FLC PSS's with MLS input to T2FLC LL SSSC controller is the least minimum value 8.0162×10^{-3} as compared to the ITAE value obtained 9.3714×10^{-3} in $\Delta\omega$ based PSS's with $\Delta\omega$ lead lag SSSC controller and ITAE obtained 11.4805×10^{-3} in $\Delta\omega$ based PSS's and ΔP based lead lag SSSC controller of the same power system.

5.3 Investigation of different contingencies in Multi-machine System:

In a multi-machine power system, the performance of the proposed SCiWOA optimized coordinated control of T2FLC PSS and T2FLC LL based SSSC damping controller can be studied under three different contingencies. (Scenario-A: three-phase fault disturbance; scenario-B: line outage; scenario-C: small disturbance)

Scenario-A: On the line between Bus-1 and Bus-6, a 3-phase fault is applied in one of the lines at a time t = 1 second.

Scenario-B: One of the lines between Bus-1 and Bus-6 is tripped off at t = 1 second.

Scenario-C: The load at bus 4 is disconnected at t = 1.0 s for 100 ms.

In the case of a 3-machine, 6-bus power system, the coordinated control of a T2FLC LL SSSC based damping controller with T2FLC PSS is considered in the same way as SMIB explained earlier. Here T2FLC PSS are considered in each machine (T2FLC PSS1, T2FLC PSS2, and T2FLC PSS3) of the system, and T2FLC LL SSSC based controller with MLC input is taken as the proposed PSS and SSSC controller. All the coordinated control parameters are obtained using the same procedure as SMIB, which is shown in Table 3. Simulation studies are conducted and discussed in various scenarios. The response of coordinated control of SSSC controller with PSS (remote input signal $\Delta\omega$ based SSSC LL and $\Delta\omega$ based PSS1, PSS2, and PSS3) is shown with dotted lines with the legend Case-1. The response of coordinated control of the SSSC controller with PSS (MLS input $\Delta\omega$ based SSSC LL and $\Delta\omega$ based PSS1, PSS2, and PSS3) is shown with dotted lines with the legend Case-2. The response of coordinated control of SSSC with the PSS proposed controller (MLS input-based T2FLC LL SSSC based controller with and $\Delta\omega$ based input T2FLC PSS1, T2FLC PSS2, and T2FLC PSS3) is shown with solid lines with the legend Case-3. Figs. 30 and 31 show the local and inter-area modes of oscillation of the response under the scenario-A coordinated control of MLS input T2FLC LL SSSC based controller with $\Delta\omega$ based input T2FLC PSS. The transient response improves better as compared to the same system in $\Delta\omega$ based PSS and MLS input to lead lag SSSC and $\Delta\omega$ based PSS and $\Delta\omega$ input to lead lag SSSC damping controller of the system. But, however, Case-2 has a better transient response as compared to Case-3. Figs. 32 and 33 show the local and inter-area modes of oscillation under scenario B, and it is clear that the proposed coordinated control of an MLS input-based SSSC controller gives a better transient response as compared to Case-2 and Case-3.

Similarly, in the scenario-C MLS input-based T2FLC PSS and T2FLC LL SSSC damping controllers, superior performance is achieved in terms of setting tine, overshoot, and undershoot as compared to the same system in the Case-2 and Case-3 coordinated controllers, which are shown in Figs. 32 and 33.

***Table 6**: SCiWOA optimized control parameters and objective function.*

Input Signal/Coordinated Control	KPS/KPPSS			T1S/ T1PSS	T2S/ T2PSS	T3S/ T3PSS	T4S/ T4PSS	J value $\times 10^{-3}$
$\Delta\omega$ based SSSC LL	17.4126			1.6027	2.0217	2.1336	0.9959	11.4805
$\Delta\omega$ based PSS1	11.5503			0.9018	2.0724	0.5373	1.9778	
$\Delta\omega$ based PSS2	32.7348			1.9647	2.3065	1.2313	2.0852	
$\Delta\omega$ based PSS3	6.5686			2.3144	2.0819	0.6492	0.5333	
MLS based SSSC LL	99.2590			1.0657	0.5338	0.4839	2.0821	9.3714
$\Delta\omega$ based PSS1	58.7825			0.1315	1.7086	1.5218	0.5499	
$\Delta\omega$ based PSS2	20.3146			1.3887	0.3198	0.4238	0.0035	
$\Delta\omega$ based PSS3	20.9087			0.4005	1.6674	0.0458	0.3001	
Input Signal/Coordinated Control	KSF1/ KPSF1	KSF2/ KpSF2	KPS/ KPPSS	T1S/ T1PSS	T2S/ T2PSS	T3S/ T3PSS	T4S/ T4PSS	J value $\times 10^{-3}$
MLS based Type-2 FLC in SSSC with LL	0.2241	0.3521	16.4629	1.2711	0.1296	0.9182	1.4624	8.0162
$\Delta\omega$ based Type-2 FLC with PSS1	0.8541	0.4673	4.6386	1.4365	0.8517	0.5490	2.2601	
$\Delta\omega$ based Type-2 FLC with PSS2	0.2302	0.5830	34.1547	1.0034	0.5132	0.5950	2.2110	
$\Delta\omega$ based Type-2 FLC with PSS3	0.0827	0.0827	46.0622	0.6055	1.4594	0.5054	0.3185	

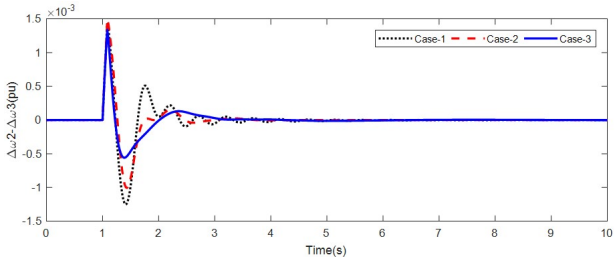

***Fig. 28**: Local area mode of oscillation under the Scenario-A.*

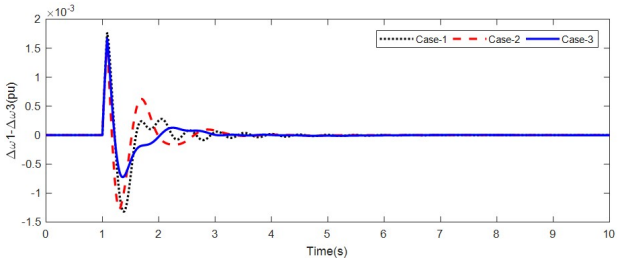

***Fig. 29**: Inter area mode of oscillation under the Scenario-A .*

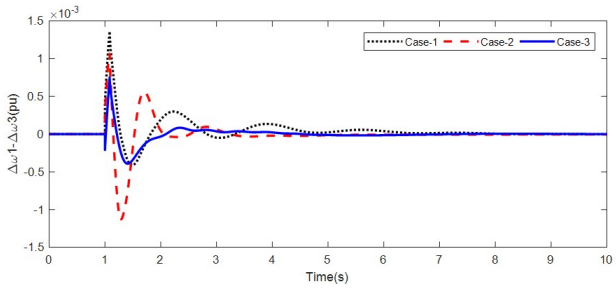

***Fig. 30**: Local area mode of oscillation under Scenario-B.*

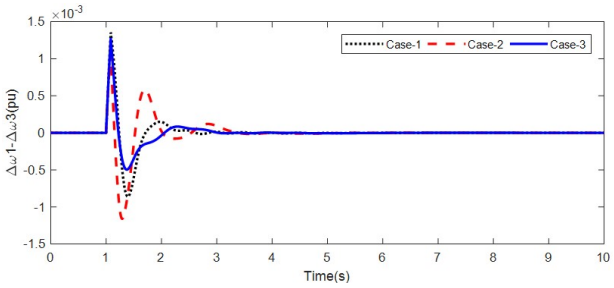

***Fig. 31**: Inter area mode of oscillation under the Scenario-B.*

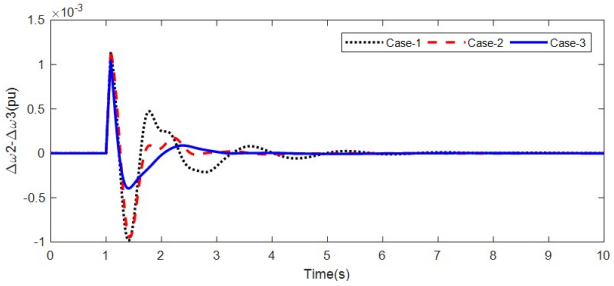

***Fig. 32**: Local area mode of oscillation under Scenario-C.*

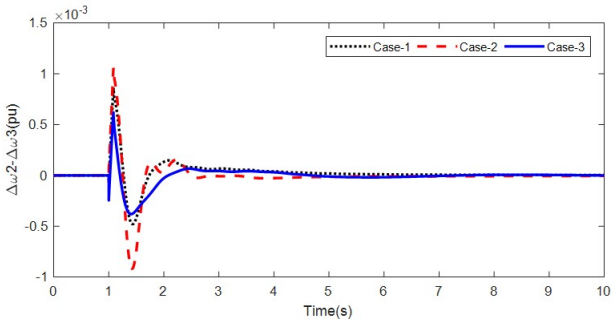

***Fig. 33**: Inter area mode of oscillation under the Scenario-C.*

6. CONCLUSION

In this study, the SCiWOA optimized coordinated control of modified input signal (MLS) based lead lag SSSC damping controller with remote speed deviation-based PSS is compared with WOA and PSO optimized

coordinated control for transient stability analysis in the same controller with the same structure of the SMIB power system. It is demonstrated by employing a SCiWOA-based design of PSS with MLS input to the lead-lag SSSC controller under different operating conditions and locations of faults in the power system for transient stability performance compared with WOA and PSO-based controllers and the same power system. It is observed that the percentage improvement in ITAE value by SCiWOA compared to WOA and PSO based optimization of the proposed system is 29.83% and 33.91%, respectively. Therefore, it can be concluded that SCiWOA based PSS with MLS input to the lead-lag SSSC controller gives better transient performances as compared to WOA and PSO based optimal design of coordinated control of PSS with MLS input to the lead-lag SSSC controller of the same power system. It is also tested under SCiWOA optimized design of coordinated control of different types of input signals to the PSS and SSSC controllers under different loading conditions and locations of faults in the SMIB power system. It is observed that $\Delta\omega$based PSS with $\Delta\omega$ based SSSC controller is a better choice for transient stability performance as compared to $\Delta\omega$ based PSS with ΔPa based SSSC controller and ΔPa based PSS with ΔPa based SSSC controller respectively. The next part of the transient stability performance analysis of the SMIB power system is the MLS input-based Type-2 FLC PSS, Type-2 FLC lead-lag SSSC based damping controller, and conventional-based PSS with PI controller demonstrated under different loading conditions. It is observed that the proposed SCiWOA optimized coordinated control MLS input-based Type-2 FLC PSS and Type-2 FLC lead lag SSSC based damping controller result in better performance in terms of settling time, overshoot, and undershoot of speed deviation as compared to three different cases (Case-1, Case-2, and Case-3) of the SMIB power system. However, Case-3 of $\Delta\omega$based PSS with MLS based SSSC and Case-2 of $\Delta\omega$based PSS with $\Delta\omega$ based SSSC coordinated of controller maintained the stability and superior performances as compared to case-1 of a conventional based PSS with a PI controller of the same power system. The effectiveness and robustness analysis of the proposed coordinated control, which can be extended to multi-machine power systems, The simulation model of three machine 6 buses with SSSC controllers and power system stabilizers is developed for demonstration of transient stability analysis. The proposed multi-machine power system of coordinated control design of a SCiWOA based Type-2 FLC PSS with a Type-2 FLC lead-lag SSSC controller was demonstrated under different fault conditions of the system. It is that the proposed Type-2 FLC SSSC coordinated controller has superior damping of low frequency oscillation performances as compared to$\Delta\omega$ based PSS and MLS based SSSC controller and $\Delta\omega$ based PSS with $\Delta\omega$ based SSSC controller under three different contingencies.

REFERENCES

[1] PW Sauer, MA Pai, *Power system dynamics and stability*, Englewood Cliffs, NJ: Prentice-Hall,1998

[2] P. Kundur, *Power System Stability and Control*, McGraw-Hill, 1994.

[3] N. G. Hingorani, L.Gyugyi, *Understanding FACTS: concepts and technology of flexible AC transmission systems*, IEEE Press, New York, 2000.

[4] L. J. Cai and I. Erlich, "Simultaneous Coordinated Tuning of PSS and FACTS Damping Controllers in Large Power Systems," *IEEE Transactions on Power Systems*, vol. 20, no. 1, pp. 294–300, Feb. 2005.

[5] . H. Chow, J. J. Sanchez-Gasca, Haoxing Ren and Shaopeng Wang, "Power system damping controller design-using multiple input signals," *IEEE Control Systems Magazine*, vol. 20, no. 4, pp. 82-90, Aug. 2000.

[6] M. Peyvandi, M. Zafarani, and E. Nasr. "Comparison of Particle Swarm Optimization and the Genetic Algorithm in the Improvement of Power System Stability by an SSSC-based Controller," *Journal of Electrical Engineering and Technology*, vol. 6, no. 2, pp. 182-191, Mar. 2011.

[7] TH. E. A. Talaat, A. Abdennour, and A. A. Al-Sulaiman, "Design and experimental investigation of a decentralized GA-optimized neuro-fuzzy power system stabilizer," *International Journal of Electrical Power & Energy Systems*, vol. 32, no. 7, pp. 751–759, Sep. 2010.

[8] M. G. Jolfaei, A. M. Sharaf, S. M. Shariatmadar, and M. B. Poudeh, "A hybrid PSS–SSSC GA-stabilization scheme for damping power system small signal oscillations," *International Journal of Electrical Power & Energy Systems*, vol. 75, pp. 337–344, Feb. 2016

[9] R.K. Khadanga and Jitendriya Ku Satapathy. "Time delay approach for PSS and SSSC based coordinated controller design using hybrid PSO– GSA algorithm", International Journal of Electrical Power & Energy Systems, Vol.71, pp.262-273 2015.

[10] S. K. Mohapatra and S. Panda, "Stability enhancement with SSSC-based controller design in presence of non-linear voltage-dependent load," *International Journal of Intelligent Systems Technologies and Applications*, vol. 15, no. 2, p. 163, 2016.

[11] G. Panda and P. K. Routray, "Gravitational Search Algorithm (GSA) Optimized SSSC Based Facts Controller to Improve Power System Oscillation Stability," *International Journal of Electrical, Computer, Energetic, Electronic and Communication Engineering*, vol. 8, no. 2, pp. 408-415, 2014.

[12] J. Belwin Edward, N. Rajasekar, K. Sathiyasekar, N. Senthilnathan, and R. Sarjila, "An enhanced bacterial foraging algorithm approach for optimal power flow problem including FACTS devices considering system loadability," *ISA Transactions*, vol. 52, no. 5, pp. 622–628, Sep. 2013.

[13] S. Panda, N. K. Yegireddy, and S. K. Mohapatra, "Hy-

brid BFOA–PSO approach for coordinated design of PSS and SSSC-based controller considering time delays," *International Journal of Electrical Power & amp; Energy Systems*, vol. 49, pp. 221–233, Jul. 2013.

[14] S. M. Abd-Elazim and E. S. Ali, "A hybrid Particle Swarm Optimization and Bacterial Foraging for optimal Power System Stabilizers design," *International Journal of Electrical Power & amp; Energy Systems*, vol. 46, pp. 334–341, Mar. 2013.

[15] S. Behera, A. K. Barisal, N. Dhal, and D. K. Lal, "Mitigation of power oscillations using hybrid DE-PSO optimization-based SSSC damping controller," *Journal of Electrical Systems and Information Technology*, vol. 6, no. 1, Dec. 2019.

[16] R. Badar and L. Khan, "Hybrid Neuro-fuzzy Legendre-based Adaptive Control Algorithm for Static Synchronous Series Compensator," *Electric Power Components and Systems*, vol. 41, no. 9, pp. 845–867, Jul. 2013.

[17] S. R. Khuntia and S. Panda, "ANFIS approach for SSSC controller design for the improvement of transient stability performance," *Mathematical and Computer Modelling*, vol. 57, no. 1–2, pp. 289–300, Jan. 2013.

[18] E. Gholipour and S. M. Nosratabadi, "A new coordination strategy of SSSC and PSS controllers in power system using SOA algorithm based on Pareto method," *International Journal of Electrical Power & amp; Energy Systems*, vol. 67, pp. 462–471, May 2015.

[19] N. Rufus, J. Calvin, Jawhar and S. Joseph, "Novel Grey Wolf Optimization Based Optimal Static Synchronous Series Compensator Design for Damping Power System Oscillations," *Journal of Computational and Theoretical Nanoscience*, vol. 15, no. 5, pp.1221-1225, 2018.

[20] P. K. Ray et al., "A Hybrid Firefly-Swarm Optimized Fractional Order Interval Type-2 Fuzzy PID-PSS for Transient Stability Improvement," *IEEE Transactions on Industry Applications*, vol. 55, no. 6, pp. 6486–6498, Nov. 2019.

[21] S. K. Mohapatra and S. Panda, "A comparative study between local and remote signal using shunt FACTS compensator-based damping controller," *International journal of Electrical Engineering and Informatics (IJEEI)*, vol. 5, no. 2, pp. 135-153, June 2013.

[22] S. Panda, S. C. Swain, and S. Mahapatra, "A hybrid BFOA–MOL approach for FACTS-based damping controller design using modified local input signal," *International Journal of Electrical Power & amp; Energy Systems*, vol. 67, pp. 238–251, May 2015.

[23] S. Mirjalili and A. Lewis, "The Whale Optimization Algorithm," *Advances in Engineering Software*, vol. 95, pp. 51–67, May 2016.

[24] D. B. Prakash and C. Lakshminarayana, "Optimal siting of capacitors in radial distribution network using Whale Optimization Algorithm," *Alexandria Engineering Journal*, vol. 56, no. 4, pp. 499–509, Dec. 2017.

[25] K. ben oualid Medani, S. Sayah, and A. Bekrar, "Whale optimization algorithm based optimal reactive power dispatch: A case study of the Algerian power system," *Electric Power Systems Research*, vol. 163, pp. 696–705, Oct. 2018.

[26] S. Mirjalili, "SCA: A Sine Cosine Algorithm for solving optimization problems," *Knowledge-Based Systems*, vol. 96, pp. 120–133, Mar. 2016.

[27] *SimPowerSystems 4.3 User's Guide*, Available: http://www.mathworks.com/products/simpower/

[28] S. K. Mohapatra, S. Panda, and P. K. Satpathy, "Power system stability improvement by static synchronous series compensator-based damping controller employing gravitational search algorithm," *International Journal of Computational Science and Engineering*, vol. 11, no. 2, pp. 143-154, Sep. 2015.

[29] M. Noroozian, G. Andersson and K. Tomsovic, "Robust, near time-optimal control of power system oscillations with fuzzy logic," *IEEE Transactions on Power Delivery*, vol. 11, no. 1, pp. 393-400, Jan. 1996.

[30] L. S. Kumar and A. Ghosh, "Modeling and control design of a static synchronous series compensator," *IEEE Transactions on Power Delivery*, vol. 14, no. 4, pp. 1448–1453, 1999.

Asit Kumar Patra graduated in Electrical Engineering in 1998 ,M.E Degree in Electrical Engineering in 2015 and Presently he is working as Assistant Professor in Electrical Engineering, Seemanta Engineering College, Mayurbhanj, Odisha and Research scholar under BPUT, Odisha. His research interests are the field of Electrical power system and control, Optimization techniques, Flexible AC Transmission System.

Sangram Keshori Mohapatra received BE degree in Electrical Engineering in the year 1999, M.Tech degree in the year of 2008 in the specialization of Power Electronics and Drives and Ph.D degree in the year of 2014 in the specialization of power system Engineering. He has acquired more than 22 years of experience in the field of Academics and Research pertaining to Electrical Engineering. Presently, he is working as an Associate Professor in Electrical Engineering, Government College of Engineering, Keonjhar a constituent college of BPUT, Odisha. He has published about 60 papers in international journal and conferences. He has guided 25 M.Tech research scholars .He is currently guiding 4 Ph.D Research scholars. He is the Life member of Indian Society for Technical Education (ISTE), India and Fellow of The Intuitions of Engineers (IEI) and member of IEEE and reviewer of various repute journal. His research interest is in the area of flexible AC transmission systems (FACTS), modeling of machines, power electronics, power systems and FACTS, controller design, power system stability, optimization Techniques. and Automatic generation and control.